Improved Moduli Backcalculation of the Upper Layers in Asphalt Pavements

Eyal Levenberg[1]; Albert Navarro[2]; and Umberto Pinori[3]

Abstract: This study was motivated by the need for improved moduli backcalculation of the upper layers in asphalt pavements. The method of improvement was to physically upgrade the usual falling weight deflectometer (FWD) design to host an extra geophone at a nontraditional offset of 100 mm, i.e., within the loading plate. A synthetic investigation was carried out first to assess the idea, which found that the extra geophone elevates the FWD's sensitivity to moduli changes in the upper portion of the pavement and offers new and meaningful deflection information. Next, device upgrades were designed and implemented in an existing FWD, transforming it to a so-called FWD_t prototype. Field testing with the new prototype demonstrated that the extra geophone measures correctly and that the added deflection data benefit backcalculation results by guiding the optimization process to distinguish between otherwise competing moduli sets. The overall conclusion is that improved moduli backcalculation, especially of the upper layers in asphalt pavements, is enabled by the FWD_t. At the same time, and given the early development stage of this device, further theoretical and experimental research is recommended to better appreciate its engineering utility. **DOI: 10.1061/JPEODX.PVENG-1527.**

Introduction

The falling weight deflectometer (FWD) is a nondestructive testing device widely used by the pavement industry [ASTM D4694-09 (ASTM 2020b); ASTM D4695-03 (ASTM 2020a)]. In simple terms, the device applies a load pulse to the tested pavement and reports the resulting surface vertical displacements (deflections) at several offset distances from the load centroid. The pulse is generated by dropping a mass onto a circular metallic plate, usually 300-mm in diameter, that is in contact with the pavement's surface. To produce a nominally uniform stress distribution, the plate is commonly partitioned into four sectors and has rubber padding at its bottom. The applied load history is measured by a load cell positioned between the falling weight and the plate, and deflection histories are obtained from the time-integration of velocity signals measured by a linear array of geophones (installed on a beam). All current FWD devices are equipped with a zero-offset geophone, measuring through a small hole in the plate's center. All other geophones are placed at offsets ranging from a minimum of 200 mm, just outside the plate's edge, up to a maximum of 2,400 mm (usually 1,800 mm).

FWD measurements are primarily aimed at assessing the in situ mechanical properties of the tested pavement (Bush and Baladi 1989; Bush et al. 1994; Tayabji and Lukanen 2000). This assessment is achieved through backcalculation, wherein layer properties in an assumed model representing the pavement system are identified by best-matching calculated deflections with deflections obtained from the geophone signals. The matching is done with optimization algorithms (Harichandran et al. 1993; Fwa et al. 1997; Park et al. 2010; Varma et al. 2013; Zhang et al. 2021; Romeo et al. 2023), while taking the layer thicknesses as a priori known to avoid an ill-conditioned problem.

For asphalt pavements, the most widely used modeling framework for backcalculation is elastostatic, based on layered elastic theory (Burmister 1945a, b, c). In brief, this theory provides a semi-analytical axisymmetric solution for a stratified half-space composed of weightless homogeneous and isotropic linear elastic layers loaded at the top boundary over a circular region (Levenberg 2020). Accordingly, the backcalculation process aims to quantify Young's moduli of the model layers (Poisson's ratios are assumed) by fitting calculated deflections under peak applied stress to deflection peaks reported by the FWD device. Although more advanced pavement modeling schemes exist (Uzan 1994; Madsen and Levenberg 2018; Lee et al. 2019), none have yet to gain widespread engineering acceptance.

Regardless of the assumed pavement model and irrespective of the chosen optimization algorithm, a successful backcalculation process is based on the premise that the FWD-reported deflections exhibit sensitivity to variation in the sought mechanical properties (assuming the signal-to-noise ratio is sufficiently high). In other words, it is challenging, if not impossible, to reliably identify a layer's modulus if a change in the modulus does not produce a measurable effect in the geophone array (Uzan 1994). For asphalt pavements, the outcome of this requirement is difficulty in evaluating the moduli of thin layers, with a thickness smaller than about one-quarter of the loading plate's diameter (Ullidtz and Coetzee 1995; Von Quintus and Killingsworth 1997; Hakim and Brown 2006).

Essentially, this difficulty refers to upper layers, given that many pavements, especially for low-volume roads, are surfaced with asphalt concrete (AC) in the thickness range of 50 mm to 100 mm, or contain relatively thin aggregate base (AB) layers (or both). This challenge also affects the reliability of backcalculation results in thick pavements when targeting the modulus of a specific AC lift or a sublayer within the AB. Such evaluations are desirable and of practical utility given that maintenance activities are often focused

[1]Associate Professor, Dept. of Environmental and Resource Engineering, The Technical Univ. of Denmark (DTU), Section for Geotechnics and Geology, Nordvej 119, Kongens Lyngby 2800, Denmark (corresponding author). ORCID: https://orcid.org/0000-0003-1188-8458. Email: eylev@dtu.dk

[2]Support & Project Manager, Dynatest A/S, Tempovej 27-29, Ballerup 2750, Denmark. Email: acs@dynatest.com

[3]Senior Pavement Engineer, Dynatest A/S, Tempovej 27-29, Ballerup 2750, Denmark. Email: upi@dynatest.com

Note. This manuscript was submitted on October 3, 2023; approved on October 29, 2024; published online on February 13, 2025. Discussion period open until July 13, 2025; separate discussions must be submitted for individual papers. This paper is part of the ***Journal of Transportation Engineering, Part B: Pavements***, © ASCE, ISSN 2573-5438.

on condition evaluation and renewal of upper pavement layers (e.g., mill-and-overlay) and less on deep reconstruction activities that affect the subbase (SB) and subgrade (SG).

In light of the above-listed challenges, this study is motivated by the need for improved moduli backcalculation of the upper layers in asphalt pavements. Herein, such improvement is not sought via advanced pavement modeling or by application of a sophisticated optimization approach (or a combination of the two); instead, it is sought through physically upgrading the usual FWD design, and specifically by adding an extra geophone at an offset of 100 mm, i.e., within the loading plate.

Subsequently, the first objective of this paper is to assess the effect of such an upgrade on the FWD's sensitivity to moduli variation in the upper layers and quantify the added information offered to the backcalculation. This is pursued in a synthetic investigation involving the simulation of different pavement systems. The second objective of this paper is to describe the design, construction, and early field validation of a new upgraded Dynatest FWD prototype tentatively named FWD_t (where the subscript t refers to "thin"). Besides the usual array of geophones, the FWD_t hosts an extra geophone at an offset of 100 mm.

Synthetic Investigation

This section presents simulation results (and analyses) based on the layered elastic code $ELLEA_1$ (version 0.96) (Levenberg et al. 2009; Levenberg 2016). Eight different five-layered systems were considered, named S1.S8 (Table 1) with Layer 1 representing AC, Layer 2 representing AB, Layer 3 representing SB, Layer 4 representing SG, and Layer 5 representing a deep soil medium. As can be seen, the top three layer thicknesses vary across the systems, while Young's moduli and Poisson's ratios are kept constant.

Specifically, layered systems S1..S4 share the same Layer 2 thickness of 150 mm and differ by the thickness of Layer 1, which varies in the range of 50 to 110 mm and by the thickness of Layer 3, which varies in the range of 240 to 300 mm. Layered systems S5..S8 share the same Layer 1 thickness of 80 mm and differ by the thickness of Layer 2, which varies in the range of 100 to 160 mm, and by the thickness of Layer 3, which varies in the range of 260 to 320 mm. It is noted that the combined thickness of the top three layers, representing the pavement structure, is kept constant at 500 mm.

All systems were loaded by a uniformly distributed vertical stress with a 0.8-MPa intensity, applied over a circular area with a 150-mm radius. This loading represents a common FWD plate under a peak load of 56.5 kN. Deflections were calculated at 10 different distances from the center of the circle, namely: $D_1 = 0$ mm, $D_2 = 100$ mm, $D_3 = 200$ mm, $D_4 = 300$ mm, $D_5 = 450$ mm, $D_6 = 600$ mm, $D_7 = 900$ mm, $D_8 = 1{,}200$ mm, $D_9 = 1{,}500$ mm, and $D_{10} = 1{,}800$ mm. The D_2 offset is nontraditional and the target of this investigation, as it resides within the loaded area.

Investigated first was deflection sensitivity to changes in moduli of the upper two layers E_1 and E_2. Based on Table 1 inputs, deflections were calculated at all 10 above-listed offsets; these calculations were repeated with E_1 increased by 1% and separately with a 1% increase in E_2. The resulting relative differences in deflections represent the FWD's sensitivity at the different geophone locations. This analysis approach quantifies the ratio of percentage change in output (i.e., deflections) to a percentage change in input (layer modulus). As such, it mimics the concept of "price elasticity of demand" in economics, which measures how sensitive the quantity demanded is to its price (Browning and Zupan 2020).

A larger relative change in deflection (in absolute value) indicates increased sensitivity and therefore improved backcalculation reliability. Conversely, a smaller relative change in deflection (in absolute value) indicates low sensitivity and thus inferior backcalculation reliability. These statements are based on the recognition that the backcalculation problem can be reliably solved only if changes in layer moduli produce a measurable effect in the deflection values. In this context, a higher FWD sensitivity means that changes in layer moduli are more strongly reflected in deflection values, and therefore chances of finding an optimal solution to the backcalculation problem are improved.

Results of this sensitivity study for layered systems S1..S4 are shown in Fig. 1 and in Fig. 2 for layered systems S5..S8. Each figure contains four charts corresponding to a different layered system; circular markers refer to E_1, while cross markers refer to E_2. The abscissas of all charts depict the $D_1..D_6$ offsets (i.e., from 0 to 600 mm). The ordinates depict sensitivities, which are primarily negative because, in general terms, a modulus increase produces a deflection decrease. Results for the new D_2 sensor (100-mm offset) are highlighted with an oval-shaped dashed line. The reason for excluding $D_7..D_{10}$ offsets from Figs. 1 and 2 is that the respective deflections are practically insensitive to E_1 and E_2.

Referring to the S1 layered system in Fig. 1(a), it can be seen (circular markers) that a 1% increase in E_1 produces a −0.10% change in deflection at D_1 (zero offset), a much smaller relative change at D_3 (200-mm offset) and a negligible effect at $D_4..D_6$. Adding the D_2 geophone (100-mm offset) improves the situation, as it can react to changes in E_1 with a sensitivity comparable to that of the D_1 geophone. Moreover, it can be seen (cross markers) that a 1% increase in E_2 produces −0.30% change in deflection at D_1, −0.20% change at D_3, −0.10% change at D_4, and almost no change at D_5 (450-mm offset) and D_6 (600-mm offset). Also in this case, adding the D_2 geophone (100-mm offset) improves the situation, as it can react to changes in E_2 with a sensitivity comparable to that of the D_1 geophone.

The sensitivity results for the S2..S4 layered systems, as shown (respectively) in Figs. 1(b–d), are essentially similar to the above-discussed. Specifically, the additional geophone at 100 mm exhibits

Table 1. Assumed properties of eight layered systems, named S1.S8, utilized for synthetically investigating the sensitivity of an FWD_t to modulus changes in the upper pavement layers

			Layer thicknesses (mm)							
Layer No.	Modulus (MPa)	Poisson	S1	S2	S3	S4	S5	S6	S7	S8
1	3,000	0.30	50	70	90	110	80	80	80	80
2	300	0.35	150	150	150	150	100	120	140	160
3	150	0.35	300	280	260	240	320	300	280	260
4	80	0.40	1,000	1,000	1,000	1,000	1,000	1,000	1,000	1,000
5	120	0.40	∝	∝	∝	∝	∝	∝	∝	∝

J. Transp. Eng., Part B: Pavements, 2025, 151(2): 04025008

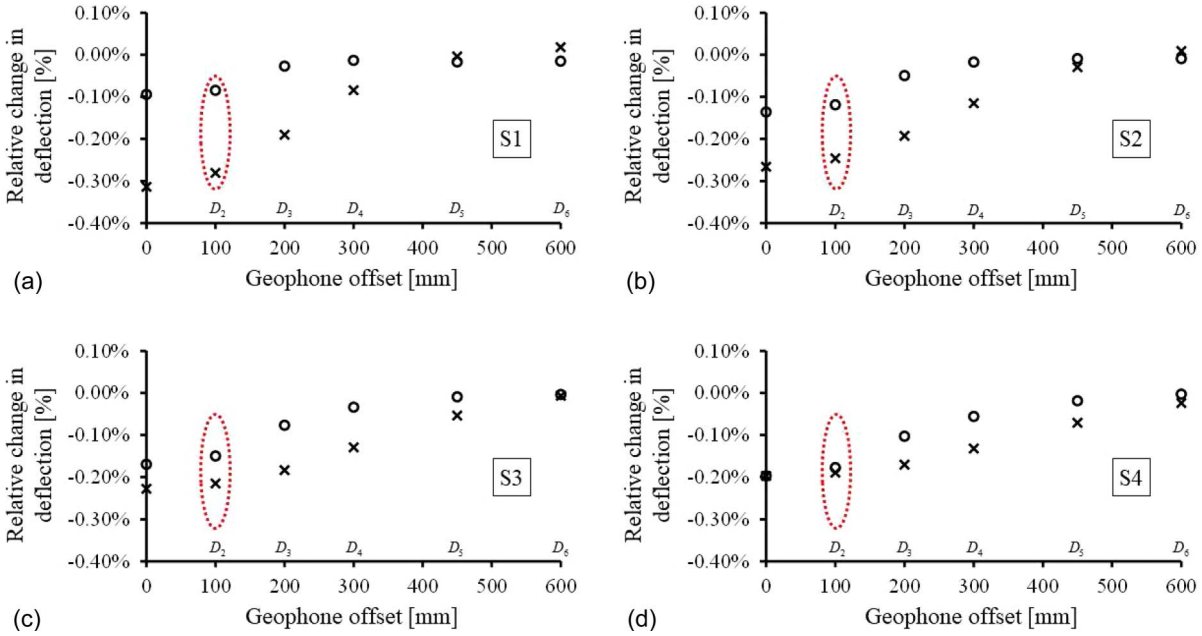

Fig. 1. Relative change in computed deflections at different offset distances for the S1..S4 layered systems (see Table 1) due to a 1% increase in the modulus value of E_1 (circular markers) and, separately, a 1% increase in the modulus value of E_2 (cross markers): (a) results for S1; (b) results for S2; (c) results for S3; and (d) results for S4.

sensitivity to changes in E_1 and E_2 comparable to the sensitivity at D_1 (zero offset) and a superior sensitivity compared to all other offsets. These results also apply to the S5..S8 layered systems, as shown in Fig. 2.

It is further noted that, across all eight charts in Figs. 1 and 2, the sensitivity to E_2 at D_1 and D_2 is generally higher than the sensitivity to E_1. This outcome seems linked to the thickness ratio between Layer 2 and Layer 1. For S1, where this ratio is three (150/50), the D_1 and D_2 sensitivities to E_2 are about three times larger than their sensitivities to E_1. For S4 and S5, where the thickness ratios between Layer 2 and Layer 1 are close to unity (100/110 and 100/80), the D_1 and D_2 sensitivities to E_1 and E_2 are comparable.

Investigated next was the new/added information offered to the backcalculation when including deflection data at a 100-mm offset. The effect sought is unrelated to the improvement in signal-to-noise ratio, which is "automatically" elevated upon adding an extra sensor to an existing sensor array. More specifically, if the deflections reported at D_2 twin those reported at D_1 or D_3 or other offsets, then no new information is added, and the backcalculation results cannot

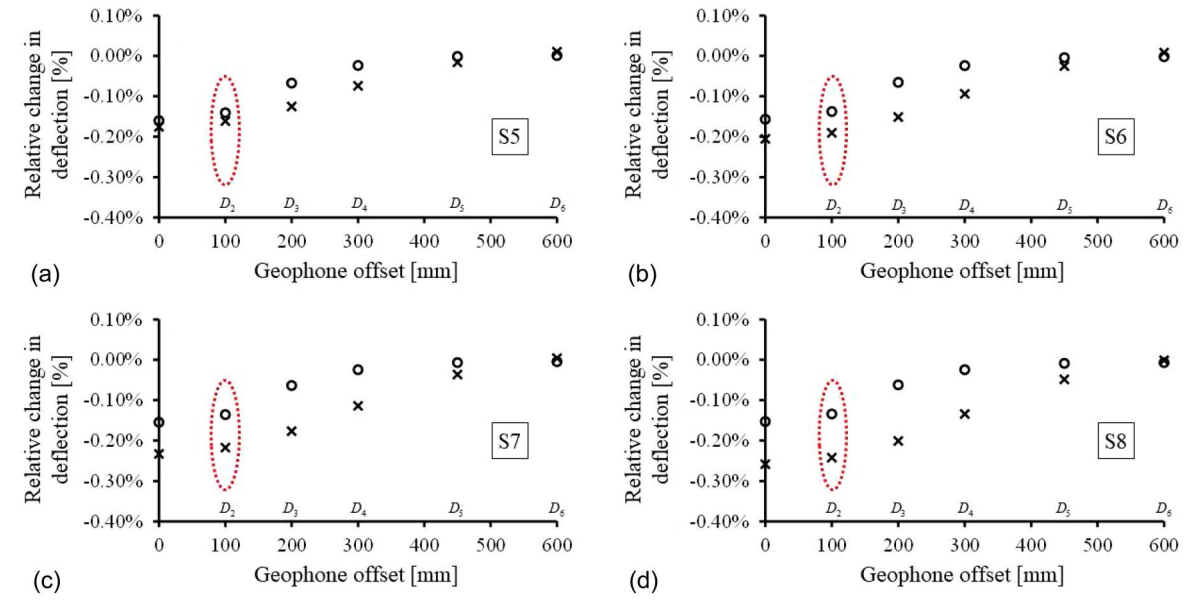

Fig. 2. Relative change in computed deflections at different offset distances for the S5..S8 layered systems (see Table 1) due to a 1% increase in the modulus value of E_1 (circular markers) and, separately, a 1% increase in the modulus value of E_2 (cross markers): (a) results for S5; (b) results for S6; (c) results for S7; and (d) results for S8.

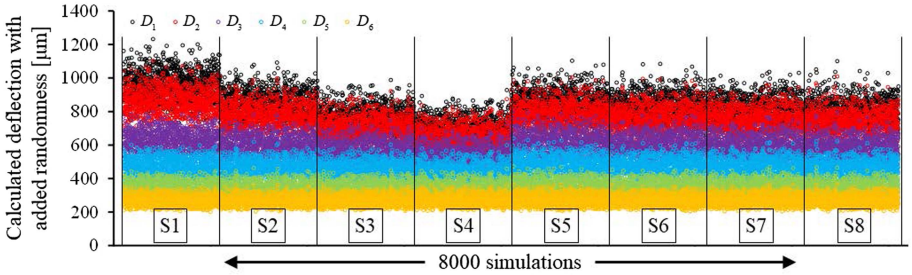

Fig. 3. Randomly generated deflection sets based on the S1..S8 layered systems (see Table 1), produced for quantifying via Eqs. (1) and (2) the added information offered to the backcalculation process by having an extra geophone at a 100-mm offset.

substantially improve despite the elevated sensitivity to changes in E_1 and E_2.

As a first step in evaluating this aspect, 1,000 deflections were simulated at $D_1..D_6$ for each of the layered systems S1..S8, producing 8,000 deflection sets in total. These deflections were produced by allowing the layer thicknesses and moduli to randomly vary about their stated values in Table 1. Utilizing a random-number generator with a zero mean and a uniform distribution function, the thicknesses were varied within ±10% and the moduli were varied within ±30%; also, noise was added to every calculated deflection value within the range of ±2 μm (Irwin et al. 1989; Neves and Cardoso 2017). The objective of this procedure was to replicate FWD measurements for dissimilar pavement systems with the added/extra geophone. Fig. 3 presents a plot of all 8,000 simulation results to graphically illustrate the type and nature of the generated data.

As a second step, statistical analysis was applied to the 8,000 deflection sets, considering the deflections at different offsets as random variables. The aim of the analysis was to quantify whether deflection data from the nonstandard offset D_2 adds new information to deflection data obtained at the other (common) offsets $D_1, D_3..D_6$. Two metrics were utilized for this purpose. The first was fraction of variance unexplained (FVU), which quantified the inability of deflections obtained at D_2 to explain the variance in deflections obtained at offsets $D_1, D_3..D_6$. The relevant formula is

$$\text{FVU} = 1 - R^2 \tag{1}$$

where R^2 = coefficient of determination, obtained by performing a simple linear regression between the D_2-deflections and the deflections at the other offsets (separately).

The second metric was mutual information (MI), which quantified the amount of information (in Hart units) derived/gained about the deflections at offsets $D_1, D_3..D_6$ from observing the D_2-deflections. An MI metric of zero indicates no mutual information, and when the mutual information approaches perfection, then MI $\to \infty$. The formula is

$$\text{MI} = -\log\left(\sqrt{1-\rho^2}\right) \tag{2}$$

where ρ = Pearson correlation coefficient, obtained from calculating the normalized covariance between the D_2-deflections and the deflections at the other offsets (separately). This MI formula embodies an intrinsic assumption that the joint distribution for the D_2-deflections and any other deflection is a bivariate normal distribution. Without such an assumption, the MI formula is somewhat convoluted and cannot be written as a simple expression (Kraskov et al. 2004; Ross 2014).

The results of the above-described calculations are presented in Fig. 4; this figure contains two charts, where the abscissa of both lists the five evaluated offset pairs and the ordinates denote the considered statistical metric (log-scale). Results of the FVU metric (in percent) are shown in Fig. 4(a); it can be seen that the D_2-deflections cannot explain about 1% the variance in the D_1-deflections and cannot explain about 10% of the variance in the D_3-deflections. For increasing deflection offsets, the unexplained variance increases toward 100%. It is noted that the FVU values for the individual layered systems, each containing 1,000 deflections (as shown in Fig. 3), exhibited similar behavior to that shown in Fig. 4(a). The values, however, were always smaller, with differences of up to 60%.

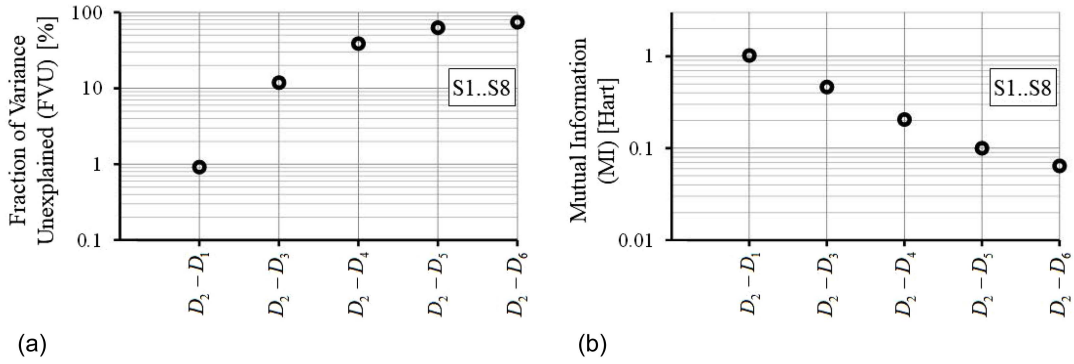

Fig. 4. The amount of new deflection information provided by a D_2 geophone (i.e., 100-mm offset) compared to common geophone offsets $D_1, D_3..D_6$ based on Fig. 3 data: (a) pairwise comparison according to the FVU metric [Eq. (1)]; and (b) pairwise comparison according to the MI metric [Eq. (2)].

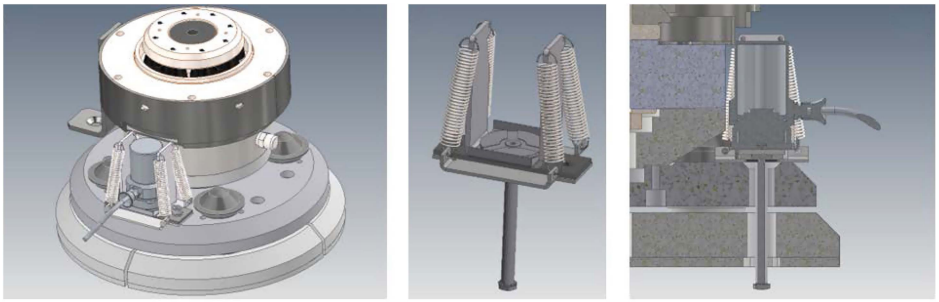

Fig. 5. Design drawings of upgrading an FWD to include an extra geophone at 100-mm offset: (a) overall assembly; (b) modified geophone holder; and (c) cross-sectional view of the installation arrangement.

Results of the MI metric are shown in Fig. 4(b), from which it can be seen that the D_2-deflections contain information about the deflections at other offsets. Most information is shared with the D_1-deflections (about 1 Hart). Qualitatively, and with reference to ρ in Eq. 2, this corresponds to a very strong correlation (Levenberg et al. 2018). The amount of information contained in the D_2-deflections about the other deflections decreases toward zero with increasing offsets. The MI values for the individual layered systems also exhibited similar behavior to that shown in Fig. 4(b). The values, however, were always larger, with differences of up to 200%.

Overall, from both abovementioned metrics, it can be stated that D_2-deflections offer new/added information to the deflections obtained at the other offsets. The addition is smallest with respect to the D_1-deflections, and increases with larger offsets. It is important to note that these findings are linked to the pavement systems assumed in Table 1, and are therefore not universal. However, the quantification approach embodied in Eqs. (1) and (2) is ubiquitous.

Device Upgrade and Testing

The task of physically upgrading the usual FWD design to include an extra geophone within the loading plate was undertaken by Dynatest A/S in early 2023. Some snips from the design drawings are shown in Fig. 5. More specifically, Fig. 5(a) presents the overall assembly, Fig. 5(b) shows an isolated view of a geophone holder, and Fig. 5(c) presents a cross-sectional view of the installation arrangement.

As shown, the holder was fixed to the top of the loading plate, allowing the newly added geophone to measure via a long pin through a small hole. The design of this holder was modified compared to the other geophone holders to provide the needed support and stability for the extra geophone (i.e., to prevent any unwanted vibrations or misalignment). The length of the center pin was designed to protrude 20 mm from the loading plate's bottom (when lifted up) to ensure sufficient tension in the holder springs during deflection measurements.

Also, as part of this upgraded design, some cuts were needed on the load cell upper flange and the welded mount ring. Last, it is noted that, due to space limitations, the 100-mm offset was oriented at right angles to the geophone beam. Given that axisymmetric models are usually assumed in the backcalculation of asphalt pavement properties, this placement is inconsequential. However, this placement is important and must be considered in the interpretation when investigating asymmetric behaviors—e.g., when targeting pavement edge effects or the transfer efficiency of joints in concrete pavements.

The above-described design upgrades were implemented onto an existing FastFWD device (Manosalvas-Paredes et al. 2017; Francesconi et al. 2020), transforming it to an FWD_t prototype. A picture offering a close view of the overall assembly, corresponding to Fig. 5(a), is shown in Fig. 6(a). A picture of the loading plate's underside is given in Fig. 6(b), where the pins of the central (D_1) and new (D_2) geophones are seen protruding through the rubber padding.

Subsequently, this FWD_t prototype was operated in test campaigns at three separate locations: (1) a parking lot surfaced with

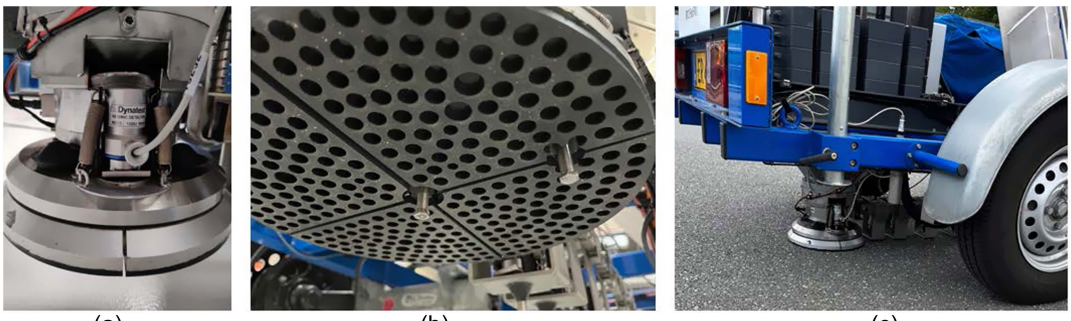

Fig. 6. Pictures of the FWD_t prototype: (a) loading plate assembly hosting an extra geophone at a 100-mm offset; (b) underside of the loading plate with protruding pins of the D_1 (central) and D_2 (new) geophones; and (c) measurement campaign over a low-volume asphalt road with a 50-mm-thick AC.

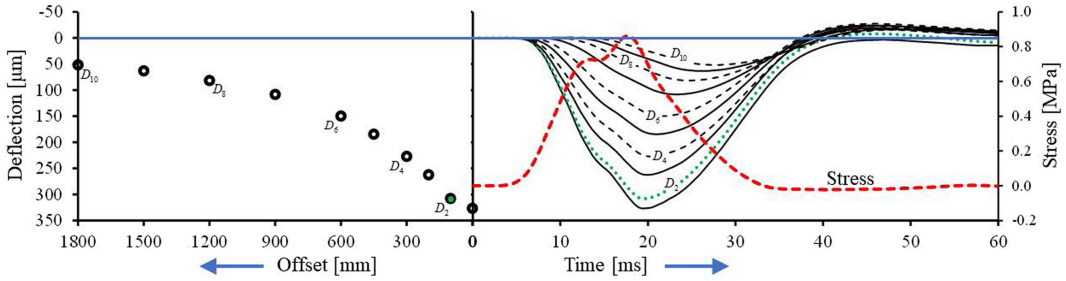

Fig. 7. Results from a single FWD_t drop at the DTU Smart Road presented as two interlinked charts of time-histories (stress and deflection) and deflection peaks.

Table 2. Deflection peaks at the DTU Smart Road: FWD_t measurements (reference), backcalculated based on all 10 available geophones, and backcalculated while excluding the D_2 data. The absolute relative errors are calculated with respect to the reference deflection peaks

		Peak deflections (μm)			Absolute relative errors (%)	
No.	Offset (mm)	FWD_t (reference)	Backcalculated with D_2 data	Backcalculated without D_2 data	With D_2 data	Without D_2 data
D_1	0	325.8	322.7	325.8	0.95	0.00
D_2	100	307.2	307.2		0.00	
D_3	200	261.9	262.0	262.5	0.06	0.26
D_4	300	226.5	226.5	226.5	0.00	0.00
D_5	450	183.9	183.9	183.8	0.01	0.04
D_6	600	149.2	151.5	151.5	1.55	1.57
D_7	900	107.6	107.6	107.6	0.00	0.00
D_8	1,200	81.2	80.7	80.6	0.62	0.74
D_9	1,500	63.0	63.3	63.2	0.36	0.21
D_{10}	1,800	51.5	51.5	51.5	0.00	0.00
Average					0.355	0.314

80-mm-thick concrete paving blocks; (2) DTU Smart Road (Nielsen and Levenberg 2023), a medium-duty asphalt road containing buried temperature and strain sensors, surfaced with 150-mm AC; and (3) a low-volume asphalt road [Fig. 6(c)] surfaced with 50-mm AC. The analysis in what follows focuses on deflection data obtained at the DTU Smart Road. This is because it had the most complete and validated information regarding layer types and thicknesses compared to the other two test locations.

The field trials aimed to provide validation for the device's upgraded design. At this development stage, the approach was to visually assess whether measurements from the extra geophone appear correct/reasonable and to provide an early evaluation of the usefulness offered by the upgrade when backcalculating field-measured data. In this context, Fig. 7 presents the FWD_t results from one drop (out of many) applied at the DTU Smart Road while the air and ride-surface temperatures were about 20°C. This figure contains two interlinked charts; the right-hand side includes time-history plots of the applied stress and reported deflections, while the left-hand side cross-plots deflection peaks and offsets. Text labels are included to help distinguish between the different lines.

For improved graphical clarity, the deflection histories are denoted by alternating solid and dashed lines, the stress history is denoted by a dashed line, and the new/nonstandard D_2 data are denoted by a dotted line. As can be seen, the latter appears correct and reasonable in terms of intensity and shape, as the D_2 data visually fall between the D_1 and D_3 data. A similar outcome was obtained under all drops performed over the DTU Smart Road and under all drops performed over the other two test locations.

The same drop height that was employed for generating Fig. 7 was repeated twice more, producing the average deflection peaks listed in Table 2; the corresponding average peak stress was 0.860 MPa. Subsequently, an elastostatic backcalculation was carried out to assess the layer moduli. For this purpose, a five-layered model was employed, with assumed thicknesses and Poisson ratios shown in Table 3. The thicknesses were based on analysis of dynamic cone penetrometer tests that were performed through the AB, SB, and SG of the DTU Smart Road, alongside construction records of the AC (Nielsen 2023). The chosen model layering corresponds to the following pavement composition (top to bottom): 150-mm AC, 250-mm AB, 500-mm SB, 600-mm SG, and local silty sand extending to a large depth.

Backcalculation was carried out with the requirement of minimizing an objective function (scalar entity) equal to the average of the individual absolute relative differences between model-calculated and FWD_t-reported deflection peaks. A gradient-descent optimization algorithm was employed for this purpose, alongside a multi-start approach to increase the likelihood of converging to a global

Table 3. Assumed five-layered model representing the DTU Smart Road pavement: Layer numbering, Poisson ratios, layer thicknesses, optimal moduli set backcalculated with all available geophones, optimal moduli set backcalculated without the D_2 data, and relative differences between the two optimal moduli sets

			Backcalculated moduli (MPa)		
Layer No.	Poisson's ratio	Thickness (mm)	With D_2 data	Without D_2 data	Relative difference (%)
1	0.30	150	5,382	4,919	−8.62
2	0.30	250	513	558	8.67
3	0.35	500	190	175	−7.63
4	0.40	600	159	177	11.87
5	0.40	∝	186	184	−1.11

minimum. The backcalculation process was carried out twice—once while considering all 10 available deflections (i.e., involving the new D_2 geophone) and a second time while disregarding the new D_2 geophone (i.e., considering only nine deflections at common offsets). The backcalculated moduli for the two cases are shown in Table 3 and the corresponding calculated deflections are shown in Table 2. As shown, and as expected, the optimal value of the objective function was larger when considering all 10 deflections (0.355%) compared to the case of ignoring the D_2 data (0.314%). At the same time, both values are very small, indicating an excellent match between model and field.

Table 3 lists the optimal moduli values obtained with and without the D_2 data. It also offers a pairwise comparison between the two moduli sets. While the two sets may be considered similar for practical purposes, it is interesting to note the effect of disregarding the D_2 geophone data: Layer 1 modulus (corresponding to AC) and Layer 3 modulus (corresponding to SB) drop by about 9%, while Layer 2 modulus (corresponding to AB) and Layer 4 modulus (corresponding to SG) increase by a comparable percentage. The modulus of Layer 5 (corresponding to a deep soil mass) was practically unaffected. These results, despite being closely linked to a specific pavement system, indicate that the addition of an extra geophone at a 100-mm offset can benefit backcalculation results by further guiding the optimization process to distinguish between competing moduli sets.

Conclusion

This study explored the idea of improving FWD backcalculation results in asphalt pavements, focusing on the upper layers. This was sought not through algorithmic advancements but by adding an extra geophone at an offset of 100 mm (i.e., within the loading plate). First, a synthetic investigation was conducted to theoretically assess the extra geophone's contribution to backcalculation. The investigation was carried out over eight different layered elastic systems (Table 1) with the dual purpose of (1) assessing the added deflection sensitivity to changes in moduli of the upper two layers, and (2) quantifying the added information offered to the backcalculation.

It was found that adding a new geophone at a 100-mm offset elevates the FWD's sensitivity to moduli changes in the upper portion of the pavement (Figs. 1 and 2). It was also found, based on two separate metrics [Eqs. (1) and (2)], that the extra geophone offers new/added information to deflections obtained at the other offsets. The information addition was small compared to the central deflection; it increased when compared to deflections obtained at larger offsets (Fig. 4). Both findings are directly linked to improved moduli backcalculation, especially of the upper layers. The improvement is over and above the elevation in the signal-to-noise ratio of the geophone array, which is "automatically" produced upon adding an extra sensor.

Next, device upgrades were designed (Fig. 5) and implemented into an existing FWD, transforming it into a so-called FWD_t prototype (Fig. 6). Through field testing with the new prototype, it was demonstrated and visually validated (Fig. 7) that the extra geophone measures correctly, and that the availability of deflection information at 100-mm offset benefits backcalculation results by guiding the optimization process to distinguish between otherwise competing moduli sets (Table 3).

The novelty of this work rests, first and foremost, in suggesting a relatively straightforward modification to the traditional FWD setup that can potentially improve its measurement performance and, thus, its engineering utility. Second, the work contains novelty in quantifying the benefit of the modification idea by borrowing concepts from economics (price elasticity of demand) and information theory (MI metric). Lastly, the work contains novelty in the manner by which the modification idea was practically implemented in an FWD prototype.

In conclusion, and based on the findings from the synthetic analyses and field tests, the FWD_t device appears to enable improved moduli backcalculation, especially of the upper layers in asphalt pavements. While this outcome is positive and promising for the pavement engineering community, further research is needed, especially given this early development stage, to help evaluate and quantify the potential utility of the new device.

First, it is recommended to gain more practical/actual testing experience with the new FWD_t and more experience with using its results for backcalculation. Second, it would be relevant to carry out deflection measurements (and subsequent backcalculation) over pavements or pavementlike media for which the layer moduli can be independently accessed by other means or are a priori known. Third, it may be worthwhile to investigate, both theoretically and experimentally, if the FWD_t design contributes to an improved evaluation of interlayer bonding conditions. Last, as this work was restricted to elastostatics, it may be of value to use the time-histories of the FWD_t, and expand the analysis into the realm of dynamic backcalculation (Madsen and Levenberg 2018; Lee et al. 2019).

Data Availability Statement

Some or all data, models, or code that support the findings of this study are available from the corresponding author upon reasonable request.

Acknowledgments

The authors would like to acknowledge the contribution and support of Matteo Pettinari for making this idea a reality and the financial support of Dynatest A/S for prototype construction and field testing.

References

ASTM. 2020a. *Standard guide for general pavement deflection measurements*. ASTM D4695-03. West Conshohocken, PA: ASTM.

ASTM. 2020b. *Standard test method for deflections with a falling-weight-type impulse load*. ASTM D4694-09. West Conshohocken, PA: ASTM.

Browning, E. K., and M. A. Zupan. 2020. *Microeconomics: Theory and applications*. 13th ed. Hoboken, NJ: Wiley.

Burmister, D. M. 1945a. "The general theory of stresses and displacements in layered systems. I." *J. Appl. Phys.* 16 (2): 89–94. https://doi.org/10.1063/1.1707558.

Burmister, D. M. 1945b. "The general theory of stresses and displacements in layered soil systems. II." *J. Appl. Phys.* 16 (3): 126–127. https://doi.org/10.1063/1.1707562.

Burmister, D. M. 1945c. "The general theory of stresses and displacements in layered soil systems. III." *J. Appl. Phys.* 16 (5): 296–302. https://doi.org/10.1063/1.1707590.

Bush, A. J., and G. Y. Baladi. 1989. *Nondestructive testing of pavements and backcalculation of moduli*. West Conshohocken, PA: ASTM.

Bush, A. J., H. L. Von Quintus, and G. Y. Baladi. 1994. *Nondestructive testing of pavements and backcalculation of moduli: Second volume*. West Conshohocken, PA: ASTM.

Francesconi, M., M. Stonecliffe-Jones, S. Khosravifar, M. Manosalvas-Paredes, A. Navarro Comes, and P. Ullidtz. 2020. "Fast falling weight deflectometer as new tool to perform accelerated pavement testing."

Proc. Inst. Civ. Eng. Transp. 173 (6): 396–409. https://doi.org/10.1680/jtran.17.00077.

Fwa, T. F., C. Y. Tan, and W. T. Chan. 1997. "Backcalculation analysis of pavement-layer moduli using genetic algorithms." *Transp. Res. Rec.* 1570 (1): 134–142. https://doi.org/10.3141/1570-16.

Hakim, B., and S. Brown. 2006. "Pavement analysis using the FWD: Practical difficulties and proposed simplifications." In Vol. 3 of *Proc., 10th Int. Conf. on Asphalt Pavements*, 1672–1681. Quebec: International Society for Asphalt Pavements.

Harichandran, R. S., T. Mahmood, A. R. Raab, and G. Y. Baladi. 1993. "Modified newton algorithm for backcalculation of pavement layer properties." *Transp. Res. Rec.* 1384: 15–22.

Irwin, L. H., W. S. Yang, and R. N. Stubstad. 1989. "Deflection reading accuracy and layer thickness accuracy in backcalculation of pavement layer moduli." In *Nondestructive testing of pavements and backcalculation of moduli*, edited by A. J. Bush III and G. Y. Baladi, 229–244. West Conshohocken, PA: ASTM.

Kraskov, A., H. Stögbauer, and P. Grassberger. 2004. "Estimating mutual information." *Phys. Rev. E* 69 (6): 066138. https://doi.org/10.1103/PhysRevE.69.066138.

Lee, H. S., D. Steele, and H. L. Von Quintus. 2019. "Who says backcalculation is only about layer moduli?" *Transp. Res. Rec.* 2673 (1): 317–331. https://doi.org/10.1177/0361198118821337.

Levenberg, E. 2016. "ELLEA1: Isotropic Layered Elasticity in Excel: Pavement analysis tool for students and engineers." Accessed October 20, 2024. https://orbit.dtu.dk/en/publications/ellea1-isotropic-layered-elasticity-in-excel-pavement-analysis-to.

Levenberg, E. 2020. *Pavement mechanics: Lecture notes*. 1st ed. Gentofte, Denmark: Eyal Levenberg.

Levenberg, E., R. S. McDaniel, and J. Olek. 2009. *Validation of NCAT structural test track experiment using INDOT APT facility.* Rep. No. FHWA/IN/JTRP-2008/26. West Lafayette, IN: Joint Transportation Research Program, Indiana DOT and Purdue Univ.

Levenberg, E., M. Pettinari, S. Baltzer, and B. M. L. Christensen. 2018. "Comparing traffic speed deflectometer and falling weight deflectometer data." *Transp. Res. Rec.* 2672 (40): 22–31. https://doi.org/10.1177/0361198118768524.

Madsen, S. S., and E. Levenberg. 2018. "Dynamic backcalculation with different load-time histories." *Road Mater. Pavement Des.* 19 (6): 1314–1333. https://doi.org/10.1080/14680629.2017.1307263.

Manosalvas-Paredes, M., A. Navarro Comes, M. Francesconi, S. Khosravifar, and P. Ullidtz. 2017. "Fast falling weight deflectometer (FASTFWD) for accelerated pavement testing (APT)." In *Bearing capacity of roads, railways and airfields*, 2235–2241. London: CRC Press.

Neves, J., and E. Cardoso. 2017. "Uncertainty evaluation of deflection measurements from fwd tests on road pavements." In *Proc., 7th Int. Conf. on Engineering Surveying: INGEO 2017*, edited by A. Kopáčik, P. Kyrinovič, and M. J. Henriques. Lisbon, Portugal: Laboratório Nacional de Engenharia Civil.

Nielsen, J. 2023. "Modeling and analysis of pavements with asphalt reinforcement: Development of a new computational model." Ph.D. dissertation, Dept. of Environmental and Resource Engineering, Technical Univ. of Denmark.

Nielsen, J., and E. Levenberg. 2023. "Full-scale validation of a mechanistic model for asphalt grid reinforcement." *Int. J. Pavement Eng.* 24 (1): 2220064. https://doi.org/10.1080/10298436.2023.2220064.

Park, S. W., H. M. Park, and J. J. Hwang. 2010. "Application of genetic algorithm and finite element method for backcalculating layer moduli of flexible pavements." *KSCE J. Civ. Eng.* 14 (2): 183–190. https://doi.org/10.1007/s12205-010-0183-8.

Romeo, R. C., R. B. Davis, H. S. Lee, S. A. Durham, and S. S. Kim. 2023. "A tandem trust-region optimization approach for ill-posed falling weight deflectometer backcalculation." *Comput. Struct.* 275 (Jan): 106935. https://doi.org/10.1016/j.compstruc.2022.106935.

Ross, B. C. 2014. "Mutual information between discrete and continuous data sets." *PloS One* 9 (2): e87357. https://doi.org/10.1371/journal.pone.0087357.

Tayabji, S. D., and E. O. Lukanen. 2000. *Nondestructive testing of pavements and backcalculation of moduli: Third volume*. West Conshohocken, PA: ASTM.

Ullidtz, P., and N. Coetzee. 1995. "Analytical procedures in nondestructive testing pavement evaluation." *Transp. Res. Rec.* 1482 (Jul): 61–66.

Uzan, J. 1994. "Advanced backcalculation techniques." In *Nondestructive testing of pavements and backcalculation of moduli: Second volume*. West Conshohocken, PA: ASTM.

Varma, S., M. E. Kutay, and E. Levenberg. 2013. "Viscoelastic genetic algorithm for inverse analysis of asphalt layer properties from falling weight deflections." *Transp. Res. Rec.* 2369 (1): 38–46. https://doi.org/10.3141/2369-05.

Von Quintus, H. L., and B. Killingsworth. 1997. *Design pamphlet for the backcalculation of pavement layer moduli in support of the 1993 AASHTO guide for the design of pavement structures*. Rep. No. FHWA-RD-97-076. McLean, VA: Office of Engineering Research and Development, Federal Highway Administration.

Zhang, X., F. Otto, and M. Oeser. 2021. "Pavement moduli back-calculation using artificial neural network and genetic algorithms." *Constr. Build. Mater.* 287 (Jun): 123026. https://doi.org/10.1016/j.conbuildmat.2021.123026.